



Phenotype- and patient-specific modelling in asthma: Bronchial thermoplasty and uncertainty quantification

Graham M. Donovan^{a,*}, David Langton^{b,c}, Peter B. Noble^d

^a Department of Mathematics, University of Auckland, Auckland 1142, New Zealand

^b Department of Thoracic Medicine, Frankston Hospital, Peninsula Health, 2 Hastings Road, Frankston, VIC 3199, Australia

^c Faculty of Medicine, Nursing and Health Sciences, Monash University, Clayton, Vic, Australia

^d School of Human Sciences, The University of Western Australia, Crawley, Western Australia, Australia

ARTICLE INFO

Article history:

Received 17 February 2020

Revised 14 May 2020

Accepted 18 May 2020

Available online 6 June 2020

Keywords:

Ventilation heterogeneity

Clustered ventilation defects

Targeted therapy

Airway hyper-responsiveness

ABSTRACT

Theoretical models can help to overcome experimental limitations to better our understanding of lung physiology and disease. While such efforts often begin in broad terms by determining the effect of a disease process on a relevant biological output, more narrowly defined simulations may inform clinical practice. Two such examples are phenotype-specific and patient-specific models, the former being specific to a group of patients with common characteristics, and the latter to an individual patient, in view of likely differences (heterogeneity) between patients. However, in order for such models to be useful, they must be sufficiently accurate, given the available data about the specific characteristics of the patient. We show that, for asthma in particular, this approach is promising: phenotype-specific targeting may be an effective way of selecting patients for treatment based on their airway remodelling phenotype, and patient-specific targeting may be viable with the use of a clinically-plausible dataset. Specifically we consider asthma and its treatment by bronchial thermoplasty, in which the airway smooth muscle layer is directly targeted by thermal energy. Patient-specific and phenotype-specific models in this context are considered using a combination of biobank data from *ex vivo* tissue samples, CT imaging, and optical coherence tomography which allows more detailed resolution of the airway wall structures.

© 2020 Elsevier Ltd. All rights reserved.

1. Introduction

Understanding of lung physiology and disease is often complicated by limitations on *in vivo* measurements. Functional measurements taken at the mouth, such as forced expiratory volume in one second or resistance, offer only an integrated assessment of overall function and cannot isolate abnormalities to specific structures or tissues. Imaging approaches such as CT or magnetic resonance imaging offer more specific information, but limited resolution means that smaller airways cannot be directly assessed (Castro et al., 2011) without extremely high energy sources which are impractical for clinical use (Dubsky et al., 2017; Murrie et al., 2020). *Ex vivo* tissue experiments offer valuable insight (e.g. Noble et al., 2013), but it is difficult to recreate the *in vivo* environment and impossible to study important interactions between airways and/or parenchyma in the integrated system. Thus mathematical models have a role to play in integrating information from these diverse sources in order to better understand lung

pathophysiology and the response to conventional and novel therapies.

All of the above is particularly true for asthma. Despite being a relatively common condition, the underlying pathophysiology is surprisingly poorly understood. While there is clearly a role for both inflammatory pathways (which result in increased airway wall thickness, amongst other things) and contraction of airway smooth muscle (ASM, activation of which transiently narrows the airways), the precise pathways involved, and relative contributions of each, are difficult to pin down (Wang et al., 2018; Elliot et al., 2018). In part this is thought to be due to the phenotypic breadth of the disease, with different features (pathologies) occurring in different cases (e.g. Wenzel, 2006; Wenzel, 2012).

The confusion around asthma extends to treatment approaches. One relatively recent therapy for asthma is *bronchial thermoplasty* (BT) which targets the ASM layer directly using radiofrequency energy delivered via bronchoscope (Cox et al., 2006). This is appealing because it targets the ASM layer directly, and thermal ablation of the ASM should result in mitigation of acute airway narrowing driven by ASM activation. However, BT is limited to a

* Corresponding author.

E-mail address: g.donovan@auckland.ac.nz (G.M. Donovan).

relatively small number of relatively large airways, while many researchers believe that smaller airways play an important role in asthma (Ueda et al., 2006). In addition, clinical trials of BT have shown consistent improvements only in patient-reported measures (such as quality-of-life questionnaire scores and rescue medication use) but not in quantitative measurements of lung function (such as forced expiratory volume in one second) (Cox et al., 2007; Pavord et al., 2007). Because the former are susceptible to the placebo effect, a sham-controlled trial was run (Castro et al., 2010), and although it reported non-placebo improvement in addition to a substantial placebo component, BT remains controversial (Laxmanan and Egressy, 2016; Iyer and Lim, 2014).

In part, this is because the underlying mechanism of action has been unclear. In an attempt to identify the underlying mechanism of BT, we employed a mathematical modelling approach to demonstrate likely changes in ventilation heterogeneity, providing an underlying mechanism of action and a possible explanation for inconsistent clinical findings (Donovan et al., 2018). This model is based on thousands of *ex vivo* tissue samples used to calibrate airway structures in different disease states (Tough et al., 1996; Hessel et al., 1999; Salkie et al., 1998; Green et al., 2010), and suggests that the underlying mechanism of action in BT is reduction in ventilation heterogeneity, which has empirical backing from hyperpolarized magnetic resonance imaging (Thomen et al., 2015). Ventilation patterns in asthma have long been known to be highly heterogeneous, with some regions of the lung over-ventilated while others are under-ventilated (Anafi and Wilson, 2001; Venegas et al., 2005); this is variously known as clustered ventilation defects, ventilation heterogeneity, or patchy ventilation. This modelling suggests that the principal benefit of BT is due to reduction in ventilation heterogeneity that results in improved long-term outcomes, and that post-BT functional improvements arise from ASM ablation in the treated central airways alone, with treatment effects propagating toward the periphery in the form of reduced ventilation heterogeneity. Moreover, this produces physiological benefit that may not be captured by routine lung function assessment but will be reflected by indirect measures of disease severity. Alternative assessment methodologies are also beginning to show non-placebo improvement in physiological observations such as airway volume assessed by CT (Langton et al., 2019a,b).

Here we are concerned with extending these findings from the generic situation, e.g. concerned with asthma only as a broad disease, into more specific settings: phenotype-specific, and patient-specific:

- *Phenotype-specific modelling.* Many different asthma phenotypes have been proposed. Here we focus on the airway remodelling phenotypes identified by Elliot et al. (2015) which can be differentiated by airway remodelling in different sized airways. (Airway remodelling is the process by which the airway wall and airway smooth muscle layers become thicker in asthma; in general, increases in remodelling result in decreases in lung function.) Specifically, Elliot et al. (2015) document three airway remodelling phenotypes in asthma: i) airway remodelling only in the large airways; ii) airway remodelling only in the small airways; and iii) airway remodelling occurring in both large and small airways. We will use a model of lung function and BT to assess the relative efficacy of BT in these structural phenotypes.
- *Patient-specific modelling.* A more distant goal is patient-specific modelling. That is, rather than placing a patient within a phenotype, and then making an assessment based on phenotype-specific modelling, it might be possible to make individual assessments based on specific information about the airway abnormalities in any one patient. In principle it may be possible,

for example, to design patient-specific targeted therapies to select which airways to treat with BT (Hall et al., 2019; Donovan et al., 2019). However, this relies critically on the availability of patient-specific data. While it may be possible to design such therapies in theory, given data of sufficient quality, it is much more challenging to do so using only data which can be plausibly collected in a clinical setting. Here we will consider the types of clinically plausible data, and their uncertainties, and how those underlying uncertainties propagate forward into uncertainty of predictions. This uncertainty quantification will help to determine the feasibility of patient-specific modelling efforts based upon these data sources.

Specifically we will consider the potential roles for CT, optical coherence tomography (OCT), polarization sensitive OCT (PS-OCT), and biobank structural data. CT is clinically common and provides information about the structure of the larger airways (principally lumen volume, airway length, and branching pattern), though cannot resolve small airways nor differentiate between different tissue types within the airway wall. OCT is more invasive, using a bronchoscope to image the airways, including airway wall thickness; a more recent development is the polarization sensitive variant, which allows differentiation between different tissue types within the airway wall, principally airway smooth muscle (Adams et al., 2016; Li et al., 2018) (see Fig. 1a). Although PS-OCT is only at the development stage, bronchoscopy is a relatively common procedure, and as such, PS-OCT is clinically plausible within the foreseeable future. However, even with OCT/PS-OCT, there are many airways which are too small (and numerous) for direct assessment in this way. Here we assume the use of biobank tissue sample data to construct a statistical model of those airways which cannot be directly measured. Thus there are several sources of uncertainty: i) measurement error from CT in the large airways (without tissue differentiation); ii) measurement error from OCT/PS-OCT in the large airways, including wall and ASM discrimination; and iii) uncertainty in the small airways due to statistical representation from biobank samples. We assess the relative contributions to the overall uncertainty of each, and thus the plausibility of patient-specific modelling based on these data sources.

2. Models and methods

We divide the presentation of the model into two sections for clarity. The underlying dynamical model considers the coupled behaviour of each airway and the subsequent evolution of flow through those airways as a network model. This is based on Donovan (2016, 2017) and the ideas of Anafi and Wilson (2001), Venegas et al. (2005) and ultimately is a system of ordinary differential equations, obtained after elimination of the algebraic side-constraints from the original system of differential-algebraic equations. The behaviour of this model is of course crucially dependent upon the airway tree structure in which these equations are solved (or more correctly, as the parameters of the system of ordinary differential equations). This model is described in Section 2.2. The airway tree structure in turn is described by its own statistical models, which describe the information about airway structure which is obtainable by CT, OCT and PS-OCT on a patient-specific basis, and also from the biobank. This is the underlying uncertainty in the inputs to be quantified in the outputs. These models are described in Section 2.1.

2.1. Airway tree structure and model domain

The geometry of the airway tree, and hence the parameters of the dynamical model, are described by a family of models for each

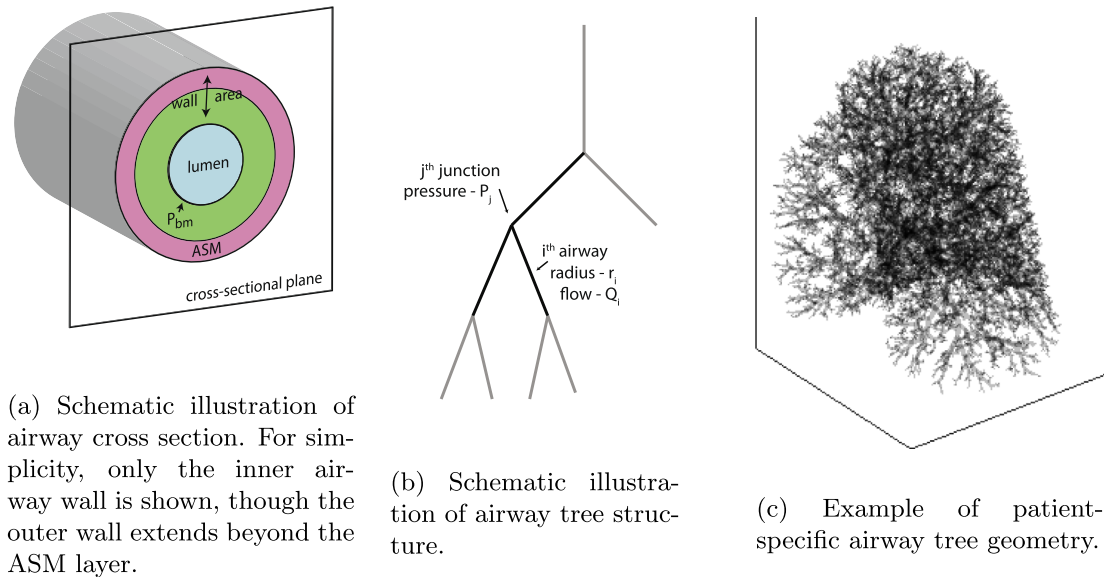


Fig. 1. Schematic illustration of model elements.

of the potential data sources: CT imaging, OCT/PS-OCT assessment via bronchoscopy, and biobank tissue sample data. Each of these models are described below.

CT. A patient-specific geometry of the large airways from Clark et al. (2014) and Hedges and Clark (2015) is used. This was obtained by use of CT imaging data to define the model geometry to the level of the first sub-segmental branches. The result of this segmentation process is a geometry of the large airways, in terms of airway radius, length, and branching geometry which we treat as ground truth. (We neglect error in the CT segmentation process; the utility of this assumption will become apparent later and discussed more fully.) Airways beyond this level were generated using a volume-filling branching algorithm (Tawhai et al., 2004). For an example, see Fig. 1c. We assume that CT is unable to reliably provide information about airway structures beyond airway radius, length, and branching geometry.

Biobank tissue samples. One way of obtaining information about the properties of the airway tree which cannot be directly assessed by imaging is to use histological examination of extensive post mortem tissue samples to calibrate a statistical model of these properties. This is the approach used in Donovan et al. (2018) and based on the Prairie Plains Asthma Study dataset (Tough et al., 1996; Hessel et al., 1999; Salkie et al., 1998; Green et al., 2010). Briefly, airways are classified by Horsfield order, which appropriately accounts for the asymmetric branching pattern of the human airway tree (Horsfield et al., 1971). Then for each airway order, and disease status, the histological dataset of 2,339 sampled airways is used to fit a tri-variate log-normal distribution describing the three key parameters for each airway: basement membrane perimeter (P_{bm}), total wall area, and ASM area¹. Fitting of these distributions is described in detail, including plots and fitted distributions, in the data supplement of ref Donovan et al. (2018). Using this statistical model, then, airway structure parameters

which cannot be directly measured on a patient-specific basis can be back-filled using population-level averages, depending on a fairly coarse-grained disease status classification: non-asthma (NA), non-fatal asthma (NFA) or fatal asthma (FA). Our definition of remodelling phenotypes is in turn based on these disease status classifications: the large airway remodelling only phenotype (LO) is based on FA airways above order 10 and NA airways below; conversely the small airway remodelling only phenotype (SO) has NA airways above threshold and FA below.

A minimal representation of the complete airway tree structure can thus be obtained by starting with the CT segmentation data for the large airways, growing the airways below the resolution threshold using a volume-filling algorithm (Tawhai et al., 2004), and then backfilling the unmeasured airway parameters using the statistical model built from the biobank data.

OCT and PS-OCT. One way to reduce this dependence on biobank data is to use additional patient-specific data obtained via conventional OCT, PS-OCT and bronchoscopy. That is, we consider a clinically-plausible procedure in which the patient undergoes bronchoscopy using OCT and PS-OCT in order to obtain airway calibre, wall area, and ASM area in each imaged airway; such a procedure will be limited to relatively large airways by the probe size, and in the number of airways imaged by time constraints. While such procedures are not performed commonly at present, the technology to do so exists, and this could be a viable clinical option. However, no direct data from a patient yet exists. As such we generate synthetic data as follows: we combine the biobank data (above) to create a synthetic ground truth for the airways to be measured, about which an estimated degree of measurement variation is imposed. Based on preliminary data (Adams et al., 2016), we estimate the measurement uncertainty at 4% standard deviation for all assessed parameters.

Data source combination. Using the representations described above, several distinct scenarios are considered. In all cases we take the initial CT data as known. In the first scenario, we imagine using CT as the only patient-specific data source, and backfilling all unmeasured parameters from the appropriate biobank-calibrated statistical model (based on population data). In the second, we imagine augmenting the initial CT segmentation with OCT and PS-OCT data for the larger airways (P_{bm} , WA, and ASM area). Clearly the first approach will have greater uncertainty; the salient ques-

¹ These quantities are traditionally expressed as cross-sectional areas, rather than thickness in three dimensions, see Fig. 1a. In intuitive terms, basement membrane perimeter sets the size of the airway, and the maximum airway calibre (as the basement membrane is inextensible). Airway wall thickening can further impinge upon the airway lumen space, restricting airflow, while the amount of ASM present determines the overall contractile capacity and hence capacity for airway narrowing when the muscle is activated.

tion is the magnitude of the reduction in uncertainty due to the inclusion of the OCT/PS-OCT measurements, and if either approach has sufficiently low uncertainty in order to be plausibly used for patient-specific therapies.

As a practical matter, the sources of uncertainty from each element above are controlled by having three distinct seeds which control the random generation of the airway tree structure: a first seed for generation of the large airway structure from biobank data, a second seed for the OCT/PS-OCT measurement error (4% standard deviation) in the large airways, and a third seed for generation of the small airway structure from biobank data. By appropriately fixing some seeds, and allowing the others to vary, different sources of uncertainty can be addressed individually.

2.2. Dynamical model

The dynamical model of airway constriction, flow conservation and pressure balance in the airway tree is based on Donovan (2017) and ideas from Anafi and Wilson (2001) and Venegas et al. (2005). We write \mathbf{r} for the vector of airway lumen radii, and \mathbf{p} and \mathbf{q} for pressure and flow vectors respectively, (see Fig. 1b) and for the i th airway we have

$$\dot{r}_i = \rho(\phi(r_i; \mathbf{r}, \mathbf{p}, \mathbf{q}) - r_i) \quad (1)$$

where ρ controls the airway relaxation time scale. The function ϕ describes static airway behaviour, e.g. $\phi = R(P_{tm}(r))$ by composition, specifically where $R(P_{tm})$ describes airway radius as a function of transmural pressure according to

$$R(P_{tm}) = \begin{cases} \sqrt{R_i^2(1 - P_{tm}/P_A)^{-n_A}}, & P_{tm} \leq 0 \\ \sqrt{r_{i\max}^2 - (r_{i\max}^2 - R_i^2)(1 - P_{tm}/P_B)^{-n_B}}, & P_{tm} > 0 \end{cases} \quad (2)$$

often called the Lambert model (Lambert et al., 1982). The parameters of Eq. (2) depend upon airway order and values are given in Donovan (2016). The function $P(r)$ gives airway transmural pressure as a function of the radius as

$$P_{tm}(r_i) = p_{mid_i} - \frac{\kappa R_{ref}}{r_i} + \tau(r_i). \quad (3)$$

where the second and third terms are the airway smooth muscle (ASM) and *parenchymal tethering* pressures. The first includes the ASM activation parameter κ , which in turn is controlled by the level of agonist dose (Donovan, 2016; Ijpm et al., 2015), and a $\propto r^{-1}$ dependence arising from the Laplace law. The second arises from the restoring forces generated by the parenchyma surrounding the airway, and is described by

$$\tau(r_i) = 2\mu_i \left(\left(\frac{R_{ref} - r_i}{R_{ref}} \right) + 1.5 \left(\frac{R_{ref} - r_i}{R_{ref}} \right)^2 \right) \quad (4)$$

according to Lai-Fook (1979). Here μ is the parenchymal shear modulus, which is dependent on lung inflation and hence provides coupling between airways via so-called *parenchymal interdependence*. Here we implement the spatially dependent shear modulus as a scattered interpolant, with the interpolant nodes are fixed at the terminal airway units, where the local inflation (and hence shear modulus) is known. Specifically, linear interpolation is used within the Delaunay triangulation of the scattered sample points to determine inflation away from the terminal units, see Donovan (2017). The parameter p_{mid_i} is the mid-airway pressure, and R_{ref} is the reference radius (Donovan, 2016).

In the conducting airways, the flow conservation constraints are

$$q_m = q_{d_1} + q_{d_2} \quad (5)$$

where the notation indicates the mother and two daughter branches at each junction. In each airway, we assume Poiseuille flow

$$\Delta p_i = \alpha_i r_i^{-4} q_i \quad (6)$$

where the constants α_i absorb all dependencies aside from radius, pressure and flow (Donovan, 2016, 2017).

This system of differential algebraic equations can be implemented generally in terms of connectivity matrices, and thus any patient-specific geometry can easily be implemented in terms of these matrices. Full details, including the details of the connectivity matrices, are given in the methods section of ref Donovan (2016).

The algebraic constraints can be eliminated by taking advantage of the linearity of pressure (Donovan, 2016). Conceptually we then have a first order system of ordinary differential equations for the airway luminal radii

$$\frac{d\vec{r}}{dt} = f(\vec{r}; \vec{C}) \quad (7)$$

where \vec{r} are the luminal radii, \vec{C} contains the airway structural parameters, and the function f now contains not just the original airway dynamics but now also incorporates the (now eliminated) algebraic constraints. These parameters, and implicitly the form of f , encode the airway tree connectivity structure as a network and can be explicitly given in terms of the airway tree connectivity matrices (Donovan, 2016). We assume a volume-controlled breathing situation, in which driving pressures are determined in order to maintain the target tidal volumes (see Donovan and Kritter, 2015). Driving pressures are constrained to the physiological range, and simulations in which tidal volumes cannot be maintained without a physical pressures are discarded; in general this occurs only at high doses of contractile agonist, and in cases of severe disease.

Resistance is calculated as the real part of impedance using a post hoc method, summing appropriately over series and parallel pathways using a Poiseuille form in each airway; these methods have been used extensively (Donovan, 2016, 2017; Donovan et al., 2018, 2019) and were originally described in Refs. Lutchen and Gillis (1997) and William Thorpe and Bates (1997).

2.3. BT treatment model

Following Donovan et al. (2018) we assume a 75% reduction in ASM in the BT treated airways and a concomitant reduction in total wall area. Non BT-treated (smaller) airways are structurally unaltered. (Note that altering the assumed level of ASM reduction does

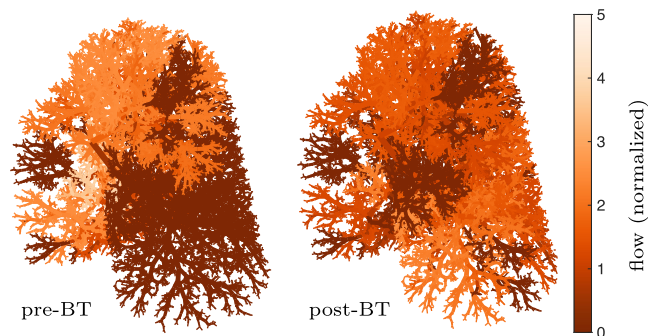


Fig. 2. Sample pair of steady state solutions; comparison between pre-BT and post-BT, where only the BT treated central airways have been structurally altered. Flow is normalized to nominal (Donovan, 2016).

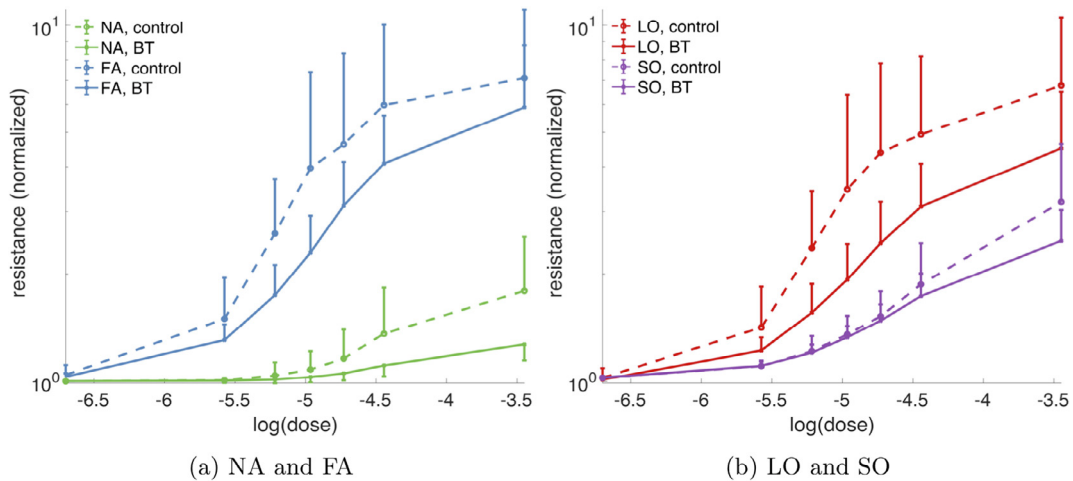


Fig. 3. Dose-response curves comparing control (pre-BT) and post-BT outcomes for non asthma (NA) and fatal asthma (FA) in panel (a), and large airway remodelling only phenotype (LO) and small airway only remodelling phenotype (SO) in panel (b). Dose is a generic ASM agonist, roughly equivalent to methacholine in terms of ASM activation according to [Ijpm et al. \(2015\)](#). Error bars show standard error.

not dramatically alter the results or underlying processes [Donovan et al., 2019](#)).

A sample simulation pair, pre-BT and post-BT at steady state, is shown in [Fig. 2](#) for an FA case at approximately 75% of maximal ASM activation. Repeating this process for different levels of ASM activation, different realizations of the structural parameters from the statistical models of structure, and also calculating the airways resistance ([Lutchen and Gillis, 1997](#)) allows a characterization of both the phenotype-specific response to BT, as well as uncertainty quantification for possible patient-specific treatments based on CT data, biobank data, and OCT/PS-OCT data.

3. Results

3.1. Phenotype-specific response: large airway remodelling vs small airway remodelling

Dose-response curves showing the response of each asthma phenotype to BT are shown in [Fig. 3](#). Here dose is a generic ASM agonist, roughly equivalent to methacholine in terms of ASM activation according to [Ijpm et al. \(2015\)](#). The FA and NA curves are as originally shown in [Donovan et al. \(2018\)](#) but are reproduced here as a useful reference comparison for the large airway remodelling only (LO) and small airway remodelling only (SO) phenotypes. In all cases, we see the characteristic response of little-to-no improvement at very low agonist dose, but progressive increases in response with both increasing dose and disease severity. These functional improvements are driven by a reduction in flow heterogeneity, which can be seen in [Fig. 2](#) for a single pair, and has been characterized more extensively using a spatial heterogeneity index in ref [Donovan et al. \(2018\)](#). The LO phenotype has a substantial BT response, as is expected with disease confined to the large airways, and a treatment which directly alters the airway structure only the large airways. The more modest improvement in the SO phenotype is perhaps also to be expected, given previous findings of downstream improvements in the small airways driven by the BT-treated large airways. This perhaps suggests that BT should be relatively favoured in the LO phenotype in comparison to other potential therapies, for example monoclonal antibody therapy ([Langton et al., 2020](#)), though that comparison also depends on the phenotype response of the other therapies. It is also interesting to note the relative severity of the LO and SO phenotypes, with the former having function levels almost comparable to FA, while SO levels are perhaps closer to NA.

3.2. Uncertainty quantification for patient-specific modelling

Using the statistical models described in [Section 2.1](#) to generate appropriate airway tree representations for each case, we can similarly assess the level of uncertainty expected in the distinct cases of using only CT and biobank data, or augmenting with OCT/PS-OCT measurements of the large airways. These cases can be further broken down into the contributions to the uncertainty from different sources.

3.2.1. CT data only

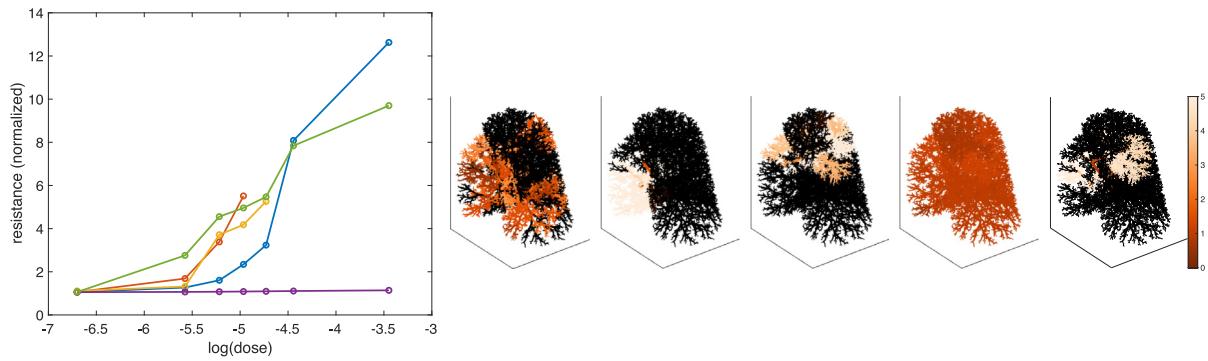
A simple assessment of the uncertainty based on using only CT and biobank data to attempt patient-specific modelling for a single FA patient is shown in [Fig. 4a](#). The left panel shows the dose-response curves for 5 independent realizations of the structural model (i.e. distinct instances of the backfilling of absent parameters from the biobank-calibrated statistical model). Sample flow patterns at $\sim 75\%$ maximal ASM activation are shown as well. Clearly here there is a great deal of variability in the response given the input uncertainty, and making useful patient-specific predictions on this basis would be challenging. While this is a small number of simulations used for easy visualisation, a more robust examination will follow. One caveat is that we have not incorporated WA measurements which may be possible from CT in the large airways, which could potentially reduce the observed uncertainty; see the Discussion.

3.2.2. CT augmented with OCT/PS-OCT

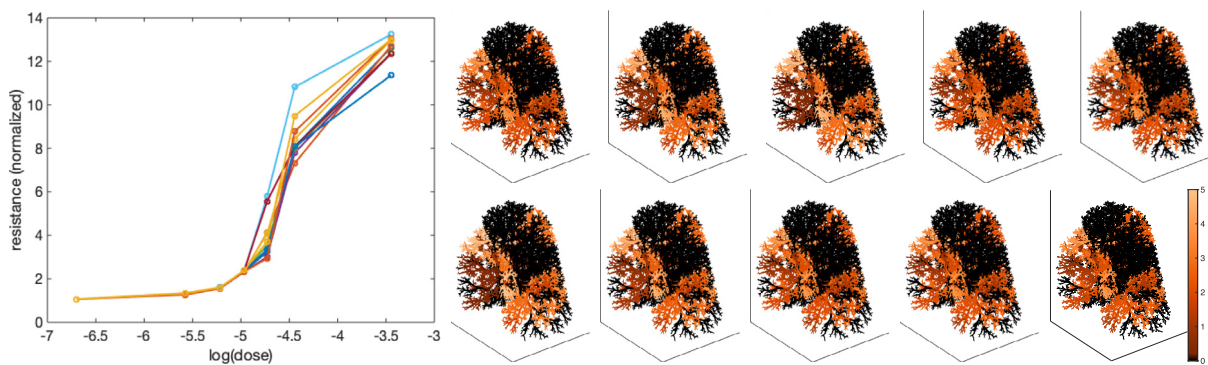
We now consider the reduction in uncertainty due to inclusion of the OCT/PS-OCT measurements in the large airways. The remaining uncertainty is then due to two sources: i) the measurement uncertainty in the PS-OCT assessed airways, and ii) the biobank backfilling uncertainty, now confined to the smaller airways.

These visualizations shown in [Fig. 4b](#) with a small number of samples suggest the relative magnitudes of the uncertainties involved. A more explicit quantification of these uncertainties, and histograms are given in [Fig. 5](#) for a much larger number of samples (500)². Panel (a) shows the overall uncertainty when using only CT and biobank data; normalizing yields a standard deviation of 0.47 – as suggested previously, probably too large to be of use in patient-specific modelling. Within panel (a), the left panel shows

² While a larger-still number of simulations might be desirable, this is currently precluded by the computational cost of approximately 1 CPU-day per simulation.



(a) Illustration of outcome variability using CT data only. Simulations in which the driving pleural pressure required to maintain flow exceed the physiological range are excluded [32].



(b) Illustration of outcome variability using CT data augmented with OCT/PS-OCT

Fig. 4. Illustration of uncertainty levels based on differing levels of input uncertainty. (a) using CT data only; (b) using CT data augmented with OCT/PS-OCT data. In each case the left-hand panel shows the family of dose-response curves, with dose in terms of $\log(\text{dose})$ of a generic agonist (e.g. methacholine) and response in terms of total resistance. The right-hand panels show the variation in the corresponding flow patterns at $\sim 75\%$ of maximum activation.

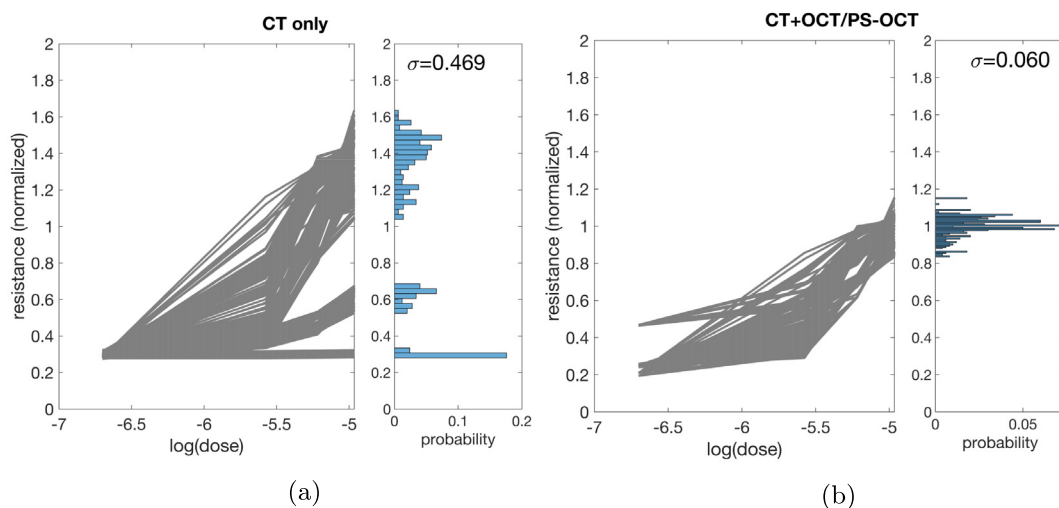


Fig. 5. Explicit histogram quantification of uncertainty for the patient-specific FA model. Panel (a): overall uncertainty assuming only CT and biobank data availability. Left hand panel shows normalized dose-response curves, while the right hand panel shows the probabilities (histogram) of outcomes at maximum dose shown. Panel (b) shows the improvement resulting from inclusion of OCT/PS-OCT data. Including OCT/PS-OCT measurements of the large airways reduces uncertainty by close to an order of magnitude.

the overlaid dose-response curves, while the smaller right-hand panel gives the probabilities of each outcome at the maximum dose shown. Panel (b) uses the same layout to illustrate the improvement when including OCT/PS-OCT data. With a normalized resistance

standard deviation of 0.06, the overall uncertainty has reduced by nearly an order of magnitude. This substantial improvement makes patient-specific modelling viable using clinically-obtainable data. Note that Fig. 5 uses a reduced maximum level of agonist stimula-

tion relative to Fig. 4a and b in order to avoid extensive loss of data due to discarded simulations in which tidal volumes cannot be maintained without aphysical driving pressures (see Section 2.2).

It is possible to further break down the sources of uncertainty; that is, in panel (b), how much of the overall uncertainty is due to the variation of the OCT/PS-OCT measurement error, and how much to the biobank data backfilling? This too can be explicitly quantified by appropriately fixing and varying the random seeds, and indeed the two sources are comparable, with the former contributing $\sigma = 0.043$ and the latter $\sigma = 0.042$. Thus the measurement uncertainty in the large airways from OCT/PS-OCT has approximately the same effect on overall uncertainty as does the biobank statistical model for the smaller airways.

4. Discussion and conclusions

We have considered the potential for phenotype-specific and patient-specific modelling of asthmatic lungs, with a particular emphasis on BT. We studied the proposed structural phenotypes of Elliot et al. (2015) in which airway remodelling may be confined to either the large airways only (LO phenotype) or small airways only (SO phenotype). In such a configuration, it is perhaps unsurprising that the LO phenotype exhibits a much greater response to BT, as BT is a treatment which directly alters the structure the large airways only. However, several aspects are notable: i) that the SO phenotype does display a small response, as is expected from the underlying mechanism of action (viz. reduction in ventilation heterogeneity propagating from the central airways to the periphery); ii) that the overall severity of the LO phenotype appears to be appreciably worse than the SO phenotype; and iii) the viability of phenotype-specific modelling to help to develop phenotype-targeted BT.

We then proceeded to consider the viability of patient-specific modelling, and the degrees of uncertainty in patient-specific modelling which can be obtained by means of different combinations of clinically-plausible data. We considered two possibilities: patient-specific modelling based on CT and biobank data only, and a version which uses OCT/PS-OCT to make direct measurements of the structural properties of the large airways, beyond what can be obtained by CT alone, rather than using biobank data to reconstruct these measurements. This analysis suggests that while relying on CT data alone as a patient-specific measurement has a large degree of uncertainty which potentially compromises the value of patient-specific predictions, the inclusion of OCT/PS-OCT measurements reduces the uncertainty by close to an order of magnitude, and forms a viable platform for patient-specific analysis. The uncertainty analysis was performed for the FA group only; while it is possible that other phenotypes would have significantly different uncertainty profiles with respect to different data sources, there is no intuitive reason to suspect that this is the case. Computational cost precludes testing all phenotypes in this way, but future studies could target selected phenotypes of interest.

There are several specific limitations which bear further scrutiny. We have assumed that CT is unable to provide an assessment of wall area. To the extent that it is possible to extract reliable wall area measurements from CT (e.g. Eddy et al., 2019), this would of course reduce the uncertainty inherent in the CT only assessment; however, not to the degree of that augmented by OCT/PS-OCT, which would provide both higher resolution of the wall area measurement in those large airways, and also discrimination of the ASM layer, which is not possible by CT. Thus a version of CT measurement, including wall area assessment in the larger airways, would be expected to lie between these two scenarios.

We have not attempted to account for variability of the ASM reduction due to BT, either on an inter-subject or intra-subject

basis, because the current evidence available on this point is not adequate to attempt to do so; indeed, even the average reductions are a subject of some contention (Brook et al., 2019; Donovan et al., 2019). However, PS-OCT has the potential to change this situation dramatically by providing relatively easy access to *in vivo* measurements of ASM (e.g. without resorting to biopsy) both before and after BT, and hence to provide a much more thorough characterization of this response. If this potential is realized it will not only settle the question of the average reduction, but also allow characterization of the variability of this response, both within and between patients.

We have also neglected any error in the CT segmentation of the large airways. This would serve to further increase the uncertainty in the CT-only approach; given the large degree of uncertainty present in that approach, this is unlikely to alter the underlying conclusions. We have also only considered the sensitivity of one particular model, where others do exist (Venegas et al., 2005; Leary et al., 2014; Roth et al., 2017; Roth et al., 2017; Chernyavsky et al., 2018; Stewart and Jensen, 2015) and may not necessarily offer the same conclusions. Nonetheless, any model which might be extended to a patient-specific setting would need to undergo some sort of uncertainty quantification, and it is probable that a similar benefit from OCT/PS-OCT inclusion might be found.

Several additional challenges loom. Other forms of patient-specific measurement might be included, especially those which indirectly reflect underlying structural properties, but from which structure might be inferred. For example, measurements of integrated function (such as the forced expiratory volume in one second) might constrain the underlying structure, but this in itself is a difficult problem (Polak et al., 2020). Similarly, hyperpolarised MRI can provide information about flow patterns (Castro et al., 2011), but the structural implications would have to be inferred. To the extent that these measures can be included, they will reduce the inherent uncertainty, but these problems remain to be addressed.

Declaration of Competing Interest

The authors declare that they have no known competing financial interests or personal relationships that could have appeared to influence the work reported in this paper.

CRedit authorship contribution statement

Graham M. Donovan: Conceptualization, Methodology, Validation, Formal analysis, Visualization, Funding acquisition. **David Langton:** Conceptualization, Writing - review & editing, Funding acquisition. **Peter B. Noble:** Conceptualization, Writing - review & editing, Funding acquisition.

References

- Adams, David C., Hariri, Lida P., Miller, Alyssa J., Wang, Yan, Cho, Josalyn L., Villiger, Martin, Holz, Jasmin A., Szabari, Margit V., Hamilos, Daniel L., Scott Harris, R., et al., 2016. Birefringence microscopy platform for assessing airway smooth muscle structure and function in vivo. *Sci. Transl. Med.* 8 (359). 359ra131–359ra131.
- Anafi, Ron C., Wilson, Theodore A., 2001. Airway stability and heterogeneity in the constricted lung. *J. Appl. Physiol.* 91 (3), 1185–1192.
- Brook, Bindi S., Chernyavsky, Igor L., Russell, Richard J., Saunders, Ruth M., Brightling, Christopher E., 2019. Comment on “unraveling a clinical paradox: why does bronchial thermoplasty work in asthma?”. *Am. J. Respiratory Cell Mol. Biol.* 61 (5), 660–661.
- Castro, Mario, Rubin, Adalberto S., Laviolette, Michel, Fiterman, Jussara, De Andrade, Marina, Lima, Pallav L., Shah, Elie Fiss, Olivenstein, Ronald, Thomson, Neil C., Niven, Robert M., et al., 2010. Effectiveness and safety of bronchial thermoplasty in the treatment of severe asthma: a multicenter, randomized,

- double-blind, sham-controlled clinical trial. *Am. J. Respiratory Crit. Care Med.* 181 (2), 116–124.
- Castro, Mario, Fain, Sean B., Hoffman, Eric A., Gierada, David S., Erzurum, Serpil C., Wenzel, Sally, 2011. Lung imaging in asthmatic patients: the picture is clearer. *J. Allergy Clin. Immunol.* 128 (3), 467–478.
- Chernyavsky, Igor L., Russell, Richard J., Saunders, Ruth M., Morris, Gavin E., Berair, Rachid, Singapur, Amisha, Chachi, Latifa, Mansur, Adel H., Howarth, Peter H., Dennison, Patrick, et al., 2018. In silico and in vivo study challenges the impact of bronchial thermoplasty on acute airway smooth muscle mass loss. *Eur. Respiratory J.* 51 (5).
- Clark, A.R., Milne, D., Wilsher, M., Burrowes, K.S., Bajaj, M., Tawhai, M.H., 2014. Lack of functional information explains the poor performance of 'clot load scores' at predicting outcome in acute pulmonary embolism. *Respiratory Physiol. Neurobiol.* 190, 1–13.
- Cox, Gerard, Miller, John D., Annette McWilliams, J., FitzGerald, Mark, Lam, Stephen, 2006. Bronchial thermoplasty for asthma. *Am. J. Respiratory Crit. Care Med.* 173 (9), 965–969.
- Cox, Gerard, Thomson, Neil C., Rubin, Adalberto S., Niven, Robert M., Corris, Paul A., Siersted, Hans Christian, Olivenstein, Ronald, Pavord, Ian D., McCormack, David, Chaudhuri, Rekha, et al., 2007. Asthma control during the year after bronchial thermoplasty. *New Engl. J. Med.* 356 (13), 1327–1337.
- Donovan, Graham M., 2016. Clustered ventilation defects and bilinear respiratory reactivity in asthma. *J. Theor. Biol.* 406, 166–175.
- Donovan, G.M., 2017. Inter-airway structural heterogeneity interacts with dynamic heterogeneity to determine lung function and flow patterns in both asthmatic and control simulated lungs. *J. Theor. Biol.* 435, 98–105.
- Donovan, Graham M., Ritter, Thibaut, 2015. Spatial pattern formation in the lung. *J. Math. Biol.* 70 (5), 1119–1149.
- Donovan, Graham M., Elliot, John G., Green, Francis H.Y., James, Alan L., Noble, Peter B., 2018. Unraveling a clinical paradox: why does bronchial thermoplasty work in asthma? *Am. J. Respiratory Cell Mol. Biol.* 59 (3), 355–362.
- Donovan, Graham M., Elliot, John G., Boser, Stacey R., Green, Francis H.Y., James, Alan L., Noble, Peter B., 2019. Patient-specific targeted bronchial thermoplasty: predictions of improved outcomes with structure-guided treatment. *J. Appl. Physiol.* 126 (3), 599–606.
- Donovan, Graham M., Elliot, John G., Green, Francis H.Y., James, Alan L., Noble, Peter B., 2019. Reply to: Comment on "unraveling a clinical paradox: Why does bronchial thermoplasty work in asthma?" Brightling. Comment on. *Am. J. Respiratory Cell Mol. Biol.* 61 (5), 661–663.
- Dubsky, Stephen, Zosky, Graeme R., Perks, Kara, Samarage, Chaminda R., Henon, Yann, Hooper, Stuart B., Fouras, Andreas, 2017. Assessment of airway response distribution and paradoxical airway dilation in mice during methacholine challenge. *J. Appl. Physiol.* 122 (3), 503–510.
- Eddy, Rachel L., Matheson, Alexander M., Svenningsen, Sarah, Knipping, Danielle, Licskai, Christopher, McCormack, David G., Parraga, Grace, 2019. Nonidentical twins with asthma: spatially matched ct airway and mri ventilation abnormalities. *Chest* 156 (6), e111–e116.
- Elliot, John G., Jones, Robyn L., Abramson, Michael J., Green, Francis H., Mauad, Thais, McKay, Karen O., Bai, Tony R., James, Alan L., 2015. Distribution of airway smooth muscle remodelling in asthma: relation to airway inflammation. *Respirology* 20 (1), 66–72.
- Elliot, John G., Noble, Peter B., Mauad, Thais, Bai, Tony R., Abramson, Michael J., McKay, Karen O., Green, Francis H.Y., James, Alan L., 2018. Inflammation-dependent and independent airway remodelling in asthma. *Respirology* 23 (12), 1138–1145.
- Green, Francis H.Y., Williams, David J., James, Alan, McPhee, Laura J., Mitchell, Ian, Mauad, Thais, 2010. Increased myoepithelial cells of bronchial submucosal glands in fatal asthma. *Thorax* 65 (1), 32–38.
- Hall, C., Quirk, J.D., Goss, C.W., Lew, D., Kozlowski, J., Thomen, R.P., Woods, J.C., Tustison, N., Mugler, J., Gallagher, L., 2019. Targeted bronchial thermoplasty guided by 129xe mri. In: B14. Late Breaking Clinical Trials. American Thoracic Society, pp. A7355–A7355.
- Hedges, Kerry L., Clark, Alys R., Tawhai, Merryn H., 2015. Comparison of generic and subject-specific models for simulation of pulmonary perfusion and forced expiration. *Interface Focus* 5 (2), 20140090.
- Hessel, Patrick A., Mitchell, Ian, Tough, Suzanne, Green, Francis H.Y., Cockcroft, Donald, Kepron, Wayne, Butt, John C., Prairie Provinces Asthma Study Group, et al., 1999. Risk factors for death from asthma. *Ann. Allergy Asthma Immunol.* 83 (5), 362–368.
- Horsfield, Keith, Dart, Gladys, Olson, Dan E., Filley, Giles F., Cumming, Gordon, 1971. Models of the human bronchial tree. *J. Appl. Physiol.* 31 (2), 207–217.
- Ijima, Gijs, Kachmar, Linda, Matusovsky, Oleg S., Bates, Jason H.T., Benedetti, Andrea, Martin, James G., Lauzon, Anne-Marie, 2015. Human trachealis and main bronchi smooth muscle are normoresponsive in asthma. *Am. J. Respiratory Crit. Care Med.* 191 (8), 884–893.
- Iyer, Vivek N., Lim, Kaiser G., 2014. Bronchial thermoplasty: reappraising the evidence (or lack thereof). *Chest* 146 (1), 17–21.
- Lai-Fook, S.J., 1979. A continuum mechanics analysis of pulmonary vascular interdependence in isolated dog lobes. *J. Appl. Physiol.* 46, 419–429.
- Lambert, R.K., Wilson, T.A., Hyatt, R.E., Rodarte, J.R., 1982. A computational model for expiratory flow. *J. Appl. Physiol.* 52, 44–56.
- Langton, D., Sloan, G., Banks, C., Bennetts, K., Plummer, V., Thien, F., 2019a. Bronchial thermoplasty increases airway volume measured by functional respiratory imaging. *Respirology Res.* 20 (1), 157.
- Langton, David, Noble, Peter B., Thien, Frank, Donovan, Graham M., 2019b. Understanding the mechanism of bronchial thermoplasty using airway volume assessed by computed tomography. *ERJ Open Res.* 5 (4).
- Langton, David, Sha, Joy, Guo, Suzy, Sharp, Julie, Banks, Ceri, Wang, Wei, Plummer, Virginia, Thien, Francis, 2020. Bronchial thermoplasty versus mepolizumab: comparison of outcomes in a severe asthma clinic. *Respirology*.
- Laxmanan, Balaji, Egressy, Katarine, Murgu, Septimiu D., White, Steven R., Kyle Hogarth, D., 2016. Advances in bronchial thermoplasty. *Chest* 150 (3), 694–704.
- Leary, Del, Winkler, Tilo, Braune, Anja, Maksym, Geoffrey N., 2014. Effects of airway tree asymmetry on the emergence and spatial persistence of ventilation defects. *J. Appl. Physiol.* 117 (4), 353–362.
- Li, Qingyun, Karnowski, Karol, Noble, Peter B., Cairncross, Alvenia, James, Alan, Villiger, Martin, Sampson, David D., 2018. Robust reconstruction of local optic axis orientation with fiber-based polarization-sensitive optical coherence tomography. *Biomed. Opt. Express* 9 (11), 5437–5455.
- Lutchen, Kenneth R., Gillis, Heather, 1997. Relationship between heterogeneous changes in airway morphometry and lung resistance and elastance. *J. Appl. Physiol.* 83 (4), 1192–1201.
- Murrie, Rhiannon P., Werdiger, Freda, Donnelley, Martin, Lin, Yu-wei, Carnibella, Richard P., Samarage, Chaminda R., Pinar, Isaac, Preissner, Melissa, Wang, Jiping, Li, Jian, et al., 2020. Real-time in vivo imaging of regional lung function in a mouse model of cystic fibrosis on a laboratory x-ray source. *Scientific Rep.* 10 (1), 1–8.
- Noble, Peter B., Jones, Robyn L., Cairncross, Alvenia, Elliot, John G., Mitchell, Howard W., James, Alan L., McFawn, Peter K., 2013. Airway narrowing and bronchodilation to deep inspiration in bronchial segments from subjects with and without reported asthma. *J. Appl. Physiol.* 114 (10), 1460–1471.
- Pavord, Ian D., Cox, Gerard, Thomson, Neil C., Rubin, Adalberto S., Corris, Paul A., Niven, Robert M., Chung, Kian F., Laviolette, Michel, 2007. Safety and efficacy of bronchial thermoplasty in symptomatic, severe asthma. *Am. J. Respiratory Crit. Care Med.* 176 (12), 1185–1191.
- Polak, Adam G., Wysoczański, Dariusz, Mrocza, Janusz, 2020. Estimation of lung properties from the forced expiration data. *IEEE Trans. Instrum. Meas.*
- Roth, Christian J., Ismail, Mahmoud, Yoshihara, Lena, Wall, Wolfgang A., 2017. A comprehensive computational human lung model incorporating inter-acinar dependencies: application to spontaneous breathing and mechanical ventilation. *Int. J. Numer. Methods Biomed. Eng.* 33 (1), e02787.
- Roth, Christian J., Yoshihara, Lena, Ismail, Mahmoud, Wall, Wolfgang A., 2017. Computational modelling of the respiratory system: discussion of coupled modelling approaches and two recent extensions. *Comput. Methods Appl. Mech. Eng.* 314, 473–493.
- Salkie, Mark L., Mitchell, Ian, Revers, Catharina W.B., Karkhanis, Arte, Butt, John, Tough, Suzanne, Green, Francis H.Y., 1998. Postmortem serum levels of tryptase and total and specific ige in fatal asthma. *Allergy and Asthma Proceedings*, vol. 19. OceanSide Publications, p. 131.
- Stewart, Peter S., Jensen, Oliver E., 2015. Patterns of recruitment and injury in a heterogeneous airway network model. *J. R. Soc. Interface* 12 (111), 20150523.
- Tawhai, Merryn H., Hunter, Peter, Tschirren, Juerg, Reinhardt, Joseph, McLennan, Geoffrey, Hoffman, Eric A., 2004. Ct-based geometry analysis and finite element models of the human and ovine bronchial tree. *J. Appl. Physiol.* 97 (6), 2310–2321.
- Thomen, Robert P., Sheshadri, Ajay, Quirk, James D., Kozlowski, Jim, Ellison, Henry D., Szczesniak, Rhonda D., Castro, Mario, Woods, Jason C., 2015. Regional ventilation changes in severe asthma after bronchial thermoplasty with 3he mr imaging and ct. *Radiology* 274 (1), 250–259.
- Tough, Suzanne C., Green, Francis H.Y., Paul, James E., Wigle, Donald T., Butt, John C., 1996. Sudden death from asthma in 108 children and young adults. *J. Asthma* 33 (3), 179–188.
- Ueda, Tetsuya, Niimi, Akio, Matsumoto, Hisako, Takemura, Masaya, Hirai, Toyohiro, Yamaguchi, Masafumi, Matsuoka, Hirofumi, Jinnai, Makiko, Muro, Shigeo, Chin, Kazuo, et al., 2006. Role of small airways in asthma: investigation using high-resolution computed tomography. *J. Allergy Clin. Immunol.* 118 (5), 1019–1025.
- Venegas, Jose G., Winkler, Tilo, Musch, Guido, Vidal, Marcos F., Melo, Dominick Layfield, Tgavalekos, Nora, Fischman, Alan J., Callahan, Ronald J., Bellani, Giacomo, Scott Harris, R., 2005. Self-organized patchiness in asthma as a prelude to catastrophic shifts. *Nature* 434 (7034), 777.
- Wang, Kimberley C.W., Le Cras, Timothy D., Larcombe, Alexander N., Zosky, Graeme R., Elliot, John G., James, Alan L., Noble, Peter B., 2018. Independent and combined effects of airway remodelling and allergy on airway responsiveness. *Clin. Sci.* 132 (3), 327–338.
- Wenzel, Sally E., 2006. Asthma: defining of the persistent adult phenotypes. *Lancet* 368 (9537), 804–813.
- Wenzel, Sally E., 2012. Asthma phenotypes: the evolution from clinical to molecular approaches. *Nat. Med.* 18 (5), 716.
- William Thorpe, C., Bates, Jason H.T., 1997. Effect of stochastic heterogeneity on lung impedance during acute bronchoconstriction: a model analysis. *J. Appl. Physiol.* 82 (5), 1616–1625.